

High dimensional optimization under non-convex excluded volume constraints

Antonio Sclocchi¹ and Pierfrancesco Urbani²

¹*Institute of Physics, École Polytechnique Fédérale de Lausanne, 1015 Lausanne, Switzerland*

²*Institut de physique théorique, Université Paris Saclay, CNRS, CEA, F-91191 Gif-sur-Yvette, France*

We consider high dimensional random optimization problems where the dynamical variables are subjected to non-convex excluded volume constraints. We focus on the case in which the cost function is a simple quadratic cost and the excluded volume constraints are modeled by a perceptron constraint satisfaction problem. We show that depending on the density of constraints, one can have different situations. If the number of constraints is small, one typically has a phase where the ground state of the cost function is unique and sits on the boundary of the island of configurations allowed by the constraints. In this case there is an hypostatic number of constraints that are marginally satisfied. If the number of constraints is increased one enters in a glassy phase where the cost function has many local minima sitting again on the boundary of the regions of allowed configurations. At the phase transition point the total number of constraints that are marginally satisfied becomes equal to the number of degrees of freedom in the problem and therefore we say that these minima are isostatic. We conjecture that increasing further the constraints the system stays isostatic up to the point where the volume of available phase space shrinks to zero. We derive our results using the replica method and we also analyze a dynamical algorithm, the Karush-Kuhn-Tucker algorithm, through dynamical mean field theory and we show how to recover the results of the replica approach in the replica symmetric phase.

I. INTRODUCTION

Several complex systems can be described by a large number of variables whose dynamics is trying to optimize some cost function under a set of constraints. In the most general setting, the cost function is arbitrary and the constraints may be either inequalities or equalities. In this work, we consider the generic situation in which there is a set of N real variables $\underline{x} = \{x_1, \dots, x_N\}$ and a set of $M = \alpha N$ inequality constraints

$$\mathcal{C} = \{g^\mu(\underline{x}) \geq 0, \mu = 1, \dots, M = \alpha N\}. \quad (1)$$

each characterized by a function $g^\mu(\underline{x})$ and we consider a cost function $H(\underline{x})$.

An example of this situation is found in classification problems in machine learning. In the simplest setting of binary classification, one has a set of inequalities that enforce the correct separation of the training set in two classes. The parameters of the machine (that correspond to the variables x_i here) must be adjusted in order to correctly satisfy these constraints. Therefore, the supervised learning task is recast into a continuous constraint satisfaction problem (CCSP). In many cases one wants to enforce that, once a solution of the problem is found, it satisfies some requirements. For example, in order to prevent numerical instabilities, one would like to have the parameters of the network to be quantities that are of the good order of magnitude and do not explode to infinity. In order to achieve this, one typically uses regularization schemes as for example Ridge regularization. In other cases, one is interested in finding sparse networks in which many of the parameters are zero. This can also be achieved by imposing an appropriate cost function on the parameters [1].

In all these cases, the machine performing the classification task is defined by the form of the functions $g_\mu(\underline{x})$

and the regularizing cost function is given by $H(\underline{x})$ which introduces some penalty to prevent that the parameters of the network behave in a way that is not the desired one. In this work we will be rather generic and we will not focus on any practical application. We will rather focus on the characterization of the landscape of the cost function H subjected to the constraints \mathcal{C} . In particular, we want to find the ground state of the cost function defined by

$$\underline{x}^* = \underset{\underline{x}: g^\mu(\underline{x}) \geq 0 \forall \mu}{\operatorname{argmin}} H(\underline{x}). \quad (2)$$

In order to have a well posed problem, we will assume that there exists a region of the phase space of \underline{x} such that all constraints are satisfied. We will call this region the SAT region (the terminology comes from constraint satisfaction problems in computer science [2]). Examples of optimization problems as Eq. (2) can be easily constructed and classified according to the properties of the corresponding cost function. We list here just a set of general cases in which the cost function is:

- *separable*: this means that each degree of freedom tries to optimize a cost function that is independent on the configuration of the other degrees of freedom. An example in this class is

$$H(\underline{x}) = \frac{1}{2} \sum_{i=1}^N (x_i - 1)^2 \quad (3)$$

but other non-convex potentials with local minima may be chosen.

- *non-separable and convex*: the cost function of each degree of freedom depends on the configuration of part or the whole system and the global cost is a convex function when it is considered in the whole

phase space (in absence of the excluded volume constraints). As an example one can consider:

$$H(\underline{x}) = \frac{1}{P} \sum_{\mu=1}^P x_i \eta_i^\mu \eta_j^\mu x_j \quad (4)$$

being η^μ i.i.d. random vectors. Another example is the following: consider the vector \underline{x} to be unconstrained. Then one wants to minimize the volume of the phase space of the vector \underline{x} , for example by minimizing $|\underline{x}|^2$, such that there is a configuration that satisfies all constraints. This problem is related to the packing problem and has been analyzed in [2–9], see also [10] for a review with the corresponding connection to deep learning.

- *non-separable and non-convex*: we have again a non-separable cost which is also non-convex. As an example, one can think of high dimensional random Gaussian functions [11]

$$H(\underline{x}) = \frac{1}{N} \sum_{i < j < k} J_{ijk} x_i x_j x_k \quad (5)$$

and the coupling constants are Gaussian variables of the order of $1/N$. In other words, one can superimpose a spin glass landscape on top of a continuous constraint satisfaction problem (CCSP) identified by the set of constraints.

This class of optimization problems is quite vast. In the following we will consider the simplest case of having a simple separable convex optimization cost and the simple set of non-convex excluded volume constraints. We will show that the non-convexity in the constraints brings about glassiness and marginal stability even when the cost function is convex by itself.

II. A TOY MODEL

In order to be concrete we consider a simple toy model. We assume that each variable x_i wants to minimize a simple convex cost function but it is constrained to be in a possibly non-convex region of phase space. We consider the simplest cost function that is

$$H(\underline{x}) = \frac{1}{2} \sum_{i=1}^N (x_i - 1)^2 \quad (6)$$

and we want to minimize it under the constraints that

$$g^\mu(\underline{x}) \geq 0, \quad \forall \mu = 1, \dots, M = \alpha N \quad (7)$$

with

$$g^\mu(\underline{x}) = \frac{1}{\sqrt{N}} \xi^\mu \cdot \underline{x} - \sigma \quad (8)$$

where $\xi^\mu = \{\xi_1^\mu, \dots, \xi_N^\mu\}$ is a random vector whose components are Gaussian random variables with zero mean and unit variance. Furthermore, we constrain \underline{x} to be on the N -dimensional sphere $|\underline{x}|^2 = N$. The constraints in Eqs. (7) and (8) define the perceptron continuous constraint satisfaction problem (CCSP). Eqs. (6), (7) and (8) define a quadratic programming problem with inequality constraints [12]. However, as we will see, the topology of the phase space and the nature of the constraints are such that the global optimization problem can become non-convex.

In [2, 3, 13, 14] the properties of the space of solutions of this CCSP have been extensively studied. As a function of σ , one has a critical value $\alpha_J(\sigma)$ of the density of constraints below which the CCSP is SAT, meaning that with probability one (for $N \rightarrow \infty$) the phase space defined by the constraints has a finite positive volume, and above which the problem is UNSAT, meaning that there is no configuration of \underline{x} that satisfies all constraints.

In the present setting we want to focus on the SAT phase. Therefore we consider $\alpha < \alpha_J(\sigma)$ and we want to optimize the cost function $H(\underline{x})$. The nature of the constraints changes completely when σ passes from being positive, where the CCSP is convex [3], to a negative value, where the solution of the CCSP lies at the intersection of non-convex domains which may be in general non-convex.

In order to study the properties of the landscape of this optimization problem, we consider the partition function defined as

$$Z = \int d\underline{x} \exp[-\beta H(\underline{x})] \left[\prod_{\mu=1}^M \theta(g^\mu(\underline{x})) \right] \quad (9)$$

where $\beta = 1/T$ is the inverse of the temperature T and $\theta(x)$ is the Heaviside step function. Given the partition function, one constructs the average free energy as

$$f = -\frac{1}{N} \overline{\ln Z} \quad (10)$$

where the overline denotes the average over the random vectors ξ s. In order to compute the properties of the landscape of the cost function, we need to study the behavior of the free energy in the zero temperature limit $\beta \rightarrow \infty$.

The average of the logarithm of the partition function can be computed using the replica method [15]

$$f = -\frac{1}{N} \lim_{n \rightarrow 0} \partial_n \overline{Z^n} \quad (11)$$

The average over the n -th power of the partition function can be obtained by considering n to be integer and then taking the analytic continuation down to $n \rightarrow 0$. Performing the integral over the random vectors ξ s (the details are essentially very close to what is reported in [2] and we will omit them) we obtain

$$\overline{Z^n} = \int d\hat{Q} \exp \left[NA(\hat{Q}) \right] \quad (12)$$

where $A(Q)$ is an action and Q is a $(n+1) \times (n+1)$ integration matrix. For $N \rightarrow \infty$ we can evaluate the integral by saddle point. The expression of the function $A(\hat{Q})$ is given by

$$A(\hat{Q}) = \frac{1}{2} \ln \det \hat{Q} - \beta(1-m) + \alpha \ln \mathcal{Z} \quad (13)$$

where we have assumed that $\hat{Q}_{1a} = \hat{Q}_{a1} = m$ independently on a . At the saddle point we have the following interpretation for the overlap matrix Q :

$$\begin{aligned} \hat{Q}_{ab} &= \frac{1}{N} \underline{x}_a \cdot \underline{x}_b & a, b > 1 \\ \hat{Q}_{1a} = \hat{Q}_{a1} &= \frac{1}{N} \sum_{i=1}^N [\underline{x}_a]_i = m & a > 1 \end{aligned} \quad (14)$$

Note that the spherical constraint on \underline{x} imposes that $\hat{Q}_{aa} = 1$. The local partition function \mathcal{Z} is given by

$$\mathcal{Z} = \exp \left[\frac{1}{2} \sum_{a,b=1}^n Q_{ab} \frac{\partial^2}{\partial h_a \partial h_b} \right] \prod_{c=1}^n \theta[h_c - \sigma] \Big|_{h=0} \quad (15)$$

where we have defined Q as the matrix obtained from \hat{Q} by removing the first row and column. The saddle point equations for the matrix \hat{Q} can be obtained in full generality following the same steps as in [2]. Here we will not repeat the computation and we will consider the replica symmetric solution and its stability.

A. The replica symmetric solution and its stability

The replica symmetric ansatz to the solution of the saddle point equations amounts to have $Q_{a \neq b} = q$ for all $a \neq b$. The order parameters m and q are then given by the following saddle point equations

$$\begin{aligned} \frac{q-m^2}{(1-q)^2} &= \alpha \int dh P(q, h) (f'(q, h))^2 \\ \frac{m}{1-q} &= \beta \end{aligned} \quad (16)$$

where

$$\begin{aligned} f(q, h) &= \ln \gamma_{1-q} \star \theta(h) \\ P(q, h) &= \gamma_q(h + \sigma) \end{aligned} \quad (17)$$

and we used the notation according to which the prime is the derivative w.r.t. h , \star denotes a convolution operation while

$$\gamma_A(h) = \frac{1}{\sqrt{2\pi A}} e^{-h^2/(2A)}. \quad (18)$$

The stability condition of the replica symmetric solution is [2, 15, 16]

$$\frac{1}{(1-q)^2} = \alpha \int dh P(q, h) (f''(q, h))^2. \quad (19)$$

When Eq. (19) is satisfied by the saddle point solution, the model enters in a glassy regime where multiple minima appear and the model is characterized by replica symmetry breaking and marginal stability [15]. The equations (16)-(19) have been derived in the finite temperature regime. However we are interested in looking at the zero temperature limit which corresponds to the ground state of the cost function. In order to take the $T \rightarrow 0$ limit we assume that in this regime

$$q = 1 - \chi T \quad T \rightarrow 0^+ \quad (20)$$

which gives $m = \chi$. Substituting this relation in the first equation of Eqs. (16) we get that χ satisfies

$$\frac{1 - \chi^2}{\chi^2} = T^2 \alpha \int dh P(1, h) (f'(1, h))^2. \quad (21)$$

Furthermore in the zero temperature limit we have

$$f(1, h) \simeq -\frac{h^2}{2\chi T} \theta(-h) \quad (22)$$

which gives

$$1 - \chi^2 = \alpha \int dh P(1, h) h^2 \theta(-h). \quad (23)$$

The stability of the RS solution is given by

$$1 = \alpha \int dh P(1, h) \theta(-h). \quad (24)$$

This relation defines the region in which replica symmetry breaking (RSB) appears. Note that Eq. (20) requires χ to be positive since q is constrained to be $q \leq 1$. The phase diagram of the model is plotted in Fig. 1 where we considered only the case of $\sigma < 0$ which gives rise to non-convex excluded volume constraints. The red line in the phase diagram represents the replica symmetric approximation for the SAT/UNSAT (jamming) transition line. Above this line there is no configuration of \underline{x} that satisfies all constraints and therefore the optimization problem makes sense only in the region below this line. This line is simply obtained by taking the $\chi \rightarrow 0$ limit of the saddle point equations. Indeed above this line no physically meaningful solution should exist. Therefore this line coincides with the one obtained in [3]. Another way to see that the $\chi \rightarrow 0$ is the right limit to get the SAT/UNSAT line is by noting that at saddle point $\chi = m$. We expect that, on this line, only one solution of the CCSP is left and, by rotational invariance of the disorder, it is orthogonal to the global minimum of the cost function. This implies that $m = 0$.

The dashed green line instead corresponds to the line that separates a strictly stable phase below it, where the ground state of the cost function is unique and not critical, from a marginally stable phase where the landscape of the cost function is glassy and local minima are marginally stable. Note that the CCSP defined by the

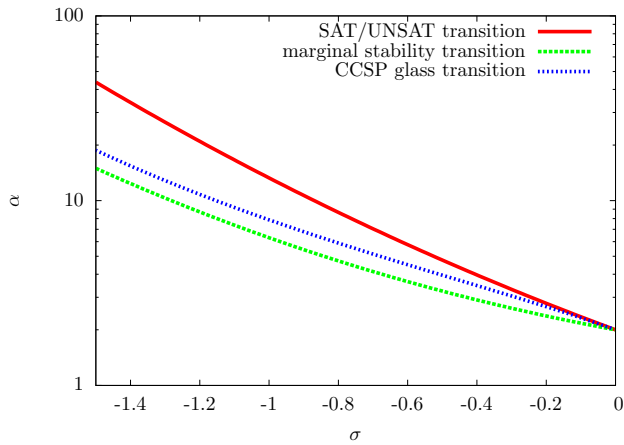


FIG. 1. The phase diagram of the toy optimization problem we are considering. The model is defined only below the SAT/UNSAT transition line for which we plotted in red the replica symmetric approximation. The SAT/UNSAT transition line represents where the volume of configurations allowed by the constraints shrinks to zero. Below the green dashed line the minimum of the cost function is unique and the replica symmetric approximation holds. Above this line instead the system enters in a glassy phase characterized by multiple minima. This phase is described by replica symmetry breaking. In the replica symmetric phase the global minimum of the cost function is characterized by a hypostatic number of marginally satisfied constraints. Upon reaching the marginal stability line the number of those constraints becomes equal to the number of degrees of freedom so that the minimum becomes isostatic. We plot in blue also the glass transition line of the perceptron CCSP. Below this line the phase space defined by the constraints is ergodic while right above ergodicity is broken and one has replica symmetry breaking.

perceptron constraints also undergoes a replica symmetry breaking transition where the space of solutions disconnects before reaching the red line. However this line, plotted also in Fig. 1, is different from the one signalling the onset of glassiness of the cost function and in particular it is closer to the SAT/UNSAT transition line. Therefore we get that *even if the CCSP is replica symmetric, the landscape of the cost function may be glassy.*

B. The distribution of gaps

In order to characterize the phase diagram, we compute the distribution of the gaps defined as the values of g^μ computed in the configuration that represents the minimum of the cost function. Using the same approach of [2], we can show that the distribution of g^μ is given by

$$\rho(h) = \frac{1}{N} \sum_{\mu=1}^M \langle \delta(h - g^\mu(\underline{x})) \rangle = c\delta(h) + \rho^+(h). \quad (25)$$

In the replica symmetric region we have that $\rho^+(h)$ is given by

$$\rho^+(h) = \alpha P(1, h) \theta(h) \quad (26)$$

and

$$c = \alpha - \alpha \int_0^\infty dh P(1, h) = \alpha \int_{-\infty}^0 dP(1, h). \quad (27)$$

Therefore, when the replica symmetric solution becomes marginally stable, the system becomes isostatic, corresponding to $c \rightarrow 1$, meaning that the number of marginally satisfied constraints equals the number of degrees of freedom in the system. At this point we may ask what happens in the glassy phase, beyond the instability line where the replica symmetric solution breaks down. We do not attempt the RSB solution of the model but we give a simple argument. At the jamming point we know that the allowed phase space of configurations shrinks to a point. This point is jamming critical and isostatic [2]. Therefore we get that at jamming as well as at the instability transition point, the system is isostatic. We therefore conjecture that the RSB phase is again isostatic and jamming critical. This would imply that we have another optimization problem for which the landscape is critical everywhere far from jamming as it happens for other cases [17–19].

III. KARUSH-KUHN-TUCKER DYNAMICS

In order to solve constrained optimization problems, one can rely on the so called Karush-Kuhn-Tucker (KKT) conditions. We consider a dynamical version of such conditions given by the following dynamical system

$$\begin{aligned} \dot{x}_i(t) &= -\zeta(t)x_i(t) - (x_i(t) - 1) \\ &+ \frac{1}{\sqrt{N}} \sum_{\mu=1}^M \xi_i^\mu f_\mu(t) \\ \dot{f}_\mu(t) &= -f_\mu(t)g_\mu(t) \end{aligned} \quad (28)$$

and $\zeta(t)$ is a Lagrange multiplier needed to enforce the spherical constraint on the variables x_i . It is simple to show that a fixed point of these equations is a solution of the optimization problem. Indeed if at long times $g_\mu > 0$, we have $f_\mu = 0$. Instead if we have $g_\mu = 0$ we have $f_\mu > 0$. The variables f_μ , that are the Lagrange multipliers of the KKT conditions, are nothing but the forces that the constraints are exerting in order to fix the corresponding variables g_μ to zero. Therefore this system of equations, when it reaches a fixed point, directly gives the statistics of forces corresponding to the g_μ that are identically equal to zero.

This set of dynamical equations can be analyzed exactly in the $N \rightarrow \infty$ limit through dynamical mean field theory. We first start by considering the case in which the dynamical system is initialized at random for the x_i

while we will fix $f_\mu(0) = 1$ which is a convenient choice. Then, in order to analyze the dynamics in the $N \rightarrow \infty$ limit, we consider the Martin-Siggia-Rose-Jensen-Dominicis dynamical path integral [11] defined as

$$Z_{\text{dyn}} = \overline{\int \mathcal{D}(\underline{f}, \hat{\underline{f}}) \mathcal{D}(\underline{x}, \hat{\underline{x}}) \mathcal{D}(\underline{r}, \hat{\underline{r}}) \exp[S_{\text{dyn}}]} \quad (29)$$

where the dynamical action is given by

$$\begin{aligned} S_{\text{dyn}} = & i \sum_{\mu=1}^M \int dt \left\{ \hat{f}_\mu(t) \left[f_\mu(t) \right. \right. \\ & \left. \left. + f_\mu(t) (r_\mu(t) - \sigma) + \hat{r}_\mu(t) r_\mu(t) \right] \right. \\ & \left. + i \sum_{i=1}^N \int dt \hat{x}_i(t) \left[\dot{x}_i + \zeta(t) x_i(t) \right. \right. \\ & \left. \left. + (x_i(t) - 1) - \frac{1}{\sqrt{N}} \sum_{\mu=1}^M \xi_i^\mu f_\mu(t) \right] \right. \\ & \left. - \frac{i}{\sqrt{N}} \sum_{i=1}^N \int dt \sum_{\mu=1}^M \hat{r}_\mu(t) \xi_i^\mu x_i(t) \right\} \end{aligned} \quad (30)$$

and the overline stands for the average over the random patterns. Taking the average over these vectors gives

$$\begin{aligned} & \overline{\exp \left[-i \sum_{\mu=1}^M \sum_{i=1}^N \xi_i^\mu \int dt (\hat{x}_i(t) f_\mu(t) + \hat{r}_\mu(t) x_i(t)) \right]} \\ & = -\frac{1}{2} \sum_{\mu=1}^M \int dt dt' [f_\mu(t) f_\mu(t') D(t, t') \\ & \quad + \hat{r}_\mu(t) \hat{r}_\mu(t') C(t, t') + 2i \hat{r}_\mu(t) f_\mu(t') R(t, t')] \end{aligned} \quad (31)$$

where we have introduced the dynamical order parameters

$$\begin{aligned} C(t, t') &= \frac{1}{N} \underline{x}(t) \cdot \underline{x}(t') \\ D(t, t') &= \frac{1}{N} \hat{\underline{x}}_i(t) \cdot \hat{\underline{x}}_i(t') \\ R(t, t') &= -\frac{1}{N} \underline{x}(t) \cdot i \hat{\underline{x}}(t') \end{aligned} \quad (32)$$

As usual, at the saddle point level $D(t, t') = 0$ by causality. The single gap effective process then gives the equation

$$r(t) = \int_0^t dt' R(t, t') f(t') + \eta(t) \quad (33)$$

where

$$\overline{\eta(t)} = 0 \quad \overline{\eta(t) \eta(t')} = C(t, t') \quad (34)$$

and

$$f(t) = \exp \left[- \int_0^t ds (r(s) - \sigma) \right] \quad (35)$$

Note that Eq.(33) must be understood as a distributional equation. Furthermore we have used that at the initial time $t = 0$ forces are initialized to $f_\mu(0) = 1$. This initialization does not affect the endpoint of the dynamics and provides a way to enforce that all forces are either zero or positive. The single site effective process is instead

$$\dot{x}(t) = -\zeta(t)x(t) - (x(t) - 1) + \Xi(t) - \int_0^t ds K(t, s)x(s) \quad (36)$$

where

$$\overline{\Xi(t)} = 0 \quad \overline{\Xi(t) \Xi(t')} = \alpha \langle f(t) f(t') \rangle = M(t, t') \quad (37)$$

and the kernel $K(t, s)$ is defined as

$$K(t, s) = \alpha \left. \frac{\delta \langle f(t) \rangle_\eta}{\delta H(t')} \right|_{H=0} \quad (38)$$

where the perturbation $H(t)$ is an additive perturbation on the right hand side of Eq. (33). Therefore we obtain the following equations for correlation, response and magnetization $m(t) = \sum_i x_i(t)/N$

$$\begin{aligned} \partial_t m(t) &= -\zeta(t)m(t) - (m(t) - 1) \\ & \quad - \int_0^t ds K(t, s)m(s) \\ \partial_t C(t, t') &= -\zeta(t)C(t, t') - (C(t, t') - m(t')) \\ & \quad - \int_0^t ds K(t, s)C(t', s) + \int_0^{t'} ds M(t, s)R(t', s) \\ \partial_t R(t, t') &= -\zeta(t)R(t, t') - R(t, t') + \delta(t - t') \\ & \quad - \int_{t'}^t ds K(t, s)R(s, t') \end{aligned} \quad (39)$$

Note that the Lagrange multiplier $\zeta(t)$ can be obtained directly from the equation for $C(t, t')$. From these dynamical equations it follows that

$$m(t) = \int_0^t ds R(t, s). \quad (40)$$

which is a relation connecting the response $R(t, s)$ function to the magnetization $m(t)$.

A. The replica symmetric solution

Let us consider what happens in the region where replica symmetry is unbroken. If we define

$$\chi = \lim_{t \rightarrow \infty} \int_0^t ds R(t, s) \quad (41)$$

we immediately have

$$m_\infty \equiv \lim_{t \rightarrow \infty} m(t) = \chi. \quad (42)$$

Considering Eq.(33) and taking the $t \rightarrow \infty$ limit we get that

$$r_\infty = \chi f_\infty + \eta \quad (43)$$

being η a normal Gaussian random variable. This equation tells us that if $f_\infty = 0$ then r_∞ is a Gaussian random variable constrained to be such that $r_\infty - \sigma$ is positive. Therefore the gap distribution is

$$P(h) = \gamma_1(h + \sigma). \quad (44)$$

On the other hand, if $r_\infty = \sigma$ then $f_\infty > 0$ and its distribution coincide with the one of the random variable $(\sigma - \eta)/\chi$ with the constraint that $\sigma - \eta > 0$. Finally we need to establish an equation for χ and show that it coincides with the one coming from the replica approach. We consider the long time limit of the equation for $m(t)$ which gives

$$0 = -\zeta_\infty \chi - (\chi - 1) - K_\infty \chi \quad (45)$$

where $K_\infty = -\alpha/\chi$. On the other hand the long time limit of the equation for M is obtained by considering the long time limit of the equation for C . This gives

$$M_\infty \chi^2 = 1 - \chi^2 \quad (46)$$

From the definition of M_∞ we finally have

$$M_\infty = \alpha \langle f_\infty^2 \rangle = \alpha \int \frac{d\eta}{\sqrt{2\pi}} e^{-\eta^2/2} \frac{(\eta + \sigma)^2}{\chi^2} \theta(\eta + \sigma) \quad (47)$$

and therefore using Eqs. (46) and (47) we get Eq. (16). This concludes the derivation of the replica symmetric equation from the KKT dynamics.

We implemented numerically the algorithm of Eq. (28) and we found that in the RS phase the algorithm goes very quickly to the solution of the optimization problem. In the RSB phase instead it seems that the algorithm does not converge and therefore we believe that in this region it makes a chaotic surf on the isostatic landscape.

IV. CONCLUSIONS

We have considered the generic setting of optimization problems under non-convex excluded volume constraints. We have analyzed a simple example of this kind in which the cost function is separable and convex and in which the non-convex excluded volume constraints are modeled by a negative perceptron.

We have found that, when the number of constraints is low enough, the cost function has a simple ground state which is captured by the replica symmetric solution of the model. At high density of constraints, instead, the optimization landscape undergoes a RSB transition where minima become marginally stable. Remarkably, we find that the RSB transition point happens *before* the point

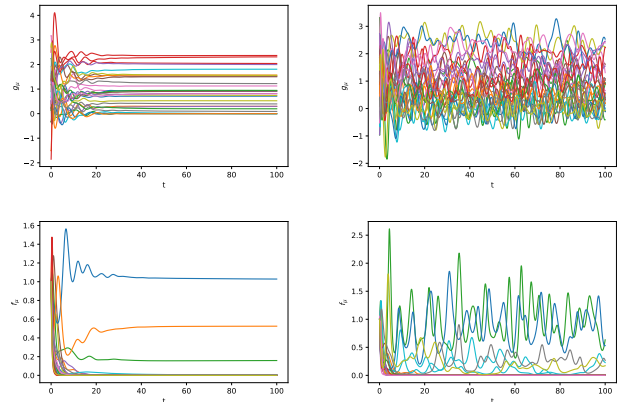


FIG. 2. Time evolution of g_μ (upper panels) and f_μ (lower panels), each color corresponding to a different $\mu = 1, \dots, 30$, obtained by numerically integrating Eq. (28) with an explicit Runge-Kutta method of order 5 [20]. The figures on left show the time evolution in the RS phase ($\alpha = 5$, $\sigma = -1$ in this example) which quickly converges to the steady state. The figures on right show the time evolution in the RSB phase ($\alpha = 8$, $\sigma = -1$ in this example): since the RSB phase is marginally stable, the time evolution is chaotic and does not converge to a stationary state. In this experiment, the f_μ have been initialized to 1 while the x_i have been initialized as standard Gaussian variables. We notice that in the steady state of the RS phase, for a given μ , $g_\mu > 0$ and $f_\mu = 0$ or $g_\mu = 0$ and $f_\mu > 0$. In this experiment we used $N = 100$.

in which the accessible phase space defined by the constraints splits into glassy regions. We have also shown how to recover these results from the dynamical mean field theory of the KKT algorithm. We leave the analysis of more complex cost functions for future work.

ACKNOWLEDGMENTS

This work was supported by "Investissements d'Avenir" LabExPALM (ANR-10-LABX-0039-PALM). A.S. thanks LPTMS where part of this work has been done.

[1] B. Neyshabur, in *Advances in Neural Information Processing Systems*, Vol. 33, edited by H. Larochelle,

M. Ranzato, R. Hadsell, M. F. Balcan, and H. Lin (Curran Associates, Inc., 2020) pp. 8078–8088.

- [2] S. Franz, G. Parisi, M. Sevelev, P. Urbani, and F. Zamponi, *SciPost Physics* **2**, 019 (2017).
- [3] S. Franz and G. Parisi, *Journal of Physics A: Mathematical and Theoretical* **49**, 145001 (2016).
- [4] S. Franz, G. Parisi, P. Urbani, and F. Zamponi, *Proceedings of the National Academy of Sciences* **112**, 14539 (2015).
- [5] H. Yoshino, *SciPost Phys* **4**, 040 (2018).
- [6] C. Brito, H. Ikeda, P. Urbani, M. Wyart, and F. Zamponi, *Proceedings of the National Academy of Sciences* **115**, 11736 (2018).
- [7] S. Franz, S. Hwang, and P. Urbani, *Physical Review Letters* **123**, 160602 (2019).
- [8] H. Ikeda, P. Urbani, and F. Zamponi, *Journal of Physics A: Mathematical and Theoretical* **52**, 344001 (2019).
- [9] H. Ikeda, *Physical Review Research* **2**, 033220 (2020).
- [10] M. Geiger, L. Petrini, and M. Wyart, *arXiv preprint arXiv:2012.15110* (2020).
- [11] T. Castellani and A. Cavagna, *Journal of Statistical Mechanics: Theory and Experiment* **2005**, P05012 (2005).
- [12] S. Boyd and L. Vandenberghe, *Convex optimization* (Cambridge university press, 2004).
- [13] E. Gardner, *Journal of physics A: Mathematical and general* **21**, 257 (1988).
- [14] E. Gardner and B. Derrida, *Journal of Physics A: Mathematical and general* **21**, 271 (1988).
- [15] M. Mézard, G. Parisi, and M. A. Virasoro, *Spin glass theory and beyond* (World Scientific, Singapore, 1987).
- [16] J. De Almeida and D. J. Thouless, *Journal of Physics A: Mathematical and General* **11**, 983 (1978).
- [17] S. Franz, A. Sclocchi, and P. Urbani, *Physical review letters* **123**, 115702 (2019).
- [18] S. Franz, A. Sclocchi, and P. Urbani, *SciPost Physics* **9**, 012 (2020).
- [19] A. Sclocchi and P. Urbani, *SciPost Phys.* **10**, 13 (2021).
- [20] J. R. Dormand and P. J. Prince, *Journal of computational and applied mathematics* **6**, 19 (1980).